African Journal of Biotechnology Vol. 11(10), pp. 2406-2416, 2 February, 2012
Available online at http://www.academicjournals.org/AJB
DOI: 10.5897/AJB10.655
ISSN 1684–5315 © 2012 Academic Journals

Review

Studies of molecular modeling on drug design of *Listeria monocytogenes* internalin B β-sheet

M. Monajjemi[1]*, E. Shirkhodaee Tari[2], F. Mollaamin[3], M. Movahedi [4] and H. Seyed Hosseini Ghaheh[5]

[1]Department of Chemistry, Science and Research Branch, Islamic Azad University, Tehran, Iran.
[2]Science and Research Branch, Islamic Azad University, Tehran, Iran.
[3]Department of Chemistry, Qom Branch, Islamic Azad University, Qom, Iran.
[4]Department of Biology, Karaj Branch, Islamic Azad University, Karaj, Iran.
[5]Young Researchers Club, Science and Research Branch, Islamic Azad University, Tehran, Iran.

Accepted 26 September, 2011

Internalin B (InlB) is an extracellular virulence factor of the bacterium *Listeria monocytogenes*, (italic) and it contains seven leucine rich repeats (LRRs) which is composed of seven β-strands aligned to form a continuous β–sheet. This β–sheet which is composed of a linear arrangement of five exposed aromatic amino acids is a hot–spot for host receptor (Met) binding and this is the goal of our studies. At first glance, the molecule were optimized with 6 to 31G (d,p) basis set in the gas phase at the Hartree–Fock (HF) level of theory. To simulate the solvent effect, the HF optimized parameters were used as initial input for subsequent HF/self–consistent reaction field (SCRF) calculations in a variety of solvents which represent a wide range of solvent properties from the point of view of polarity, as well as the hydrogen bond donor and acceptor strength, implementing 6 to 31G (d,p) atomic basis set. For deeper investigations of β–sheet folding, thermodynamic signatures of this biomolecule as an island of cooperatively–ordered hydrogen–bonded network by calculating Gibbs free energy and enthalpy were determined. Four different temperatures that this bacterium may encounter in the environment, and in cold-blooded animals or warm-blooded hosts in three solvent media were used. Then, NMR studies was carried out on the basis of gauge-including atomic orbital (GIAO) method at HF/6–31G (d,p) level of theory, to gain more insight to solvent effects on aromatic amino acids ^{15}N and ^{17}O atoms shielding in order to probe InlB–Met (ligand–protein) binding via clarifying of chemical shift mapping and dynamics.

Key words: Internalin B, β–sheet (un) folding, thermodynamics, solvent effect, nuclear magnetic resonance.

INTRODUCTION

In the last few years, a variety of *ab initio* computational calculations have been developed for better understanding of energetic properties, charge distributions, bond values, magnetic shielding, thermodynamics and others that are not readily available.

Bacterial virulence factors show a striking abundance of repetitive sequences including leucine rich repeat (LRR) domains (Cabanes et al., 2002). They mediate protein-protein interactions fundamental to many biological processes such as signalling, cell adhesion, enzyme modulation, intracellular transport and plant disease resistance (Pishkar et al., 2010; Mollaamin et al., 2010). The families of internalin proteins from *Listeria monocytogenes* contain a highly regular LRR domain. Invasiveness of this bacterium for mediating systemic infection is a trait that is acquired after the ability of attaching, internalizing and spreading in the several tissues and cell types of eukaryotic host cells expressing Met receptor such as epithelial, endothelial, hepatic cells and fibroblasts. These characters are induced by Internalin B (InlB), a *Listeria* surface-associated virulence protein (Chatterjee et al., 2006; Cossart, 2002; Cossart et al., 2003). The three-dimensional crystal structure of the InlB has been determined by X-ray crystallography.

*Corresponding author. E-mail: m_monajjemi@yahoo.com.

It has a modular architecture comprised of an N-terminal cap domain, a LRR domain of 22 amino acid repeats and an inter-repeat region (IR) domain followed by a second repeat region that non–covalently anchors the protein to the bacterial cell wall.

So in addition to the bacterial-bound form of InlB, a main part of it, is released into the medium as a soluble molecule. Hence, we envisage that its secretion into the medium or localization at the bacterial surface requires a considerable stability against chemical and thermal denaturation (Khodayari et al., 2010; Marino et al., 2000). In fact, β–sheet is distributed across the entire LRR domain and harbored a linear array of five substantial aromatic amino acids (F104, W124, F126, Y170 and Y214) dispensable for the InlB–mediated invasion of *Listeria* into mammalian cells. These residues are positioned in close proximity and constitute a single binding site. The sequence alignment of other internalin LRRs represents the most variability of these exposed residues on the concave face of molecule which is an indicative of the importance of this region in receptor binding (Machner et al., 2003; Shen et al., 2000). Since high-affinity binding events between LRR and Met are necessary for internalization of bacteria, it is desired to understand the energetic and structural details of such interactions.

Due to the modular structure and repetitive feature of InlB, it can be trimmed into smaller fragments that remain folded. Moreover, the elongated β–sheet in the whole LRR domain involves inter-repeated hydrogen bonding, spanning over all seven repeats. The architectural results of a local topology without the long-range contacts that typify most globular proteins and are unique to the pathogenic *Listeria* strains (Khodayari et al., 2010; Schubert et al., 2001) when taken together, have made it an appropriate biomolecule model to better understand biochemical and biophysical properties among similar structural elements even by computational methods. The kinetics and thermodynamics of InlB and β–sheet folding have traditionally been studied by optical spectroscopies, calorimetry and scattering techniques (Schubert et al., 2001; Courtemanche and Barrick, 2008).

Although, these techniques provide crucial information about global structural transitions, it also provide relatively little and direct information about site–specific structural features particularly at the atomic levels. So, this study allows to comparing energy distribution and stability between β–strands and residue-specific analysis in a monomeric β–sheet via *ab initio* calculations. Compared to α-helical repeat proteins, the folding of repeat proteins containing β–sheet structure have not been extensively investigated (Freiberg et al., 2004). On the other hand, no *ab initio* studies have been reported on repeat proteins containing β–sheets, especially with the characteristic of InlB β–sheet yet.

One area where thermodynamics can be useful, is in the process of protein (un)folding and binding between a macromolecule and a ligand (Mollaamin et al., 2010). These calculations specially in appreciating the strength and specificity of noncovalent intra and intermolecular interactions, contributing to the protein stability and ligand–receptor properties are carried out in the gas phase incorporating with environmental effect via solvent continuum. Present methodological approaches using modest computational facilities in conjunction with the solvent representation given by self-consistent reaction field (SCRF) model, provide a powerful tool to investigating the extent of hydrogen-bonding and polarity/polarisability properties of the solvent and its influence on the physicochemical quantities especially in compounds and interactions that solvation effects cannot be neglected (Monajjemi and Chahkandi, 2005; Patel et al., 1999). For more structural determination, *ab initio* multinuclear NMR calculations using the “gauge–including atomic orbital” (GIAO) method were performed in various solvents. Atoms in different environments experience different amount of shielding. These calculations on truncated model systems can predict reasonable chemical shift values and have became a powerful tool in understanding the variations in the molecular structure and functions as well as the role of them in drug design (Monajjemi et al., 2005). Moreover, many NMR studies especially in drug design and pharmacology, are of homologous proteins (Donald and Martin, 2009), and it has been determined that LRR domains are predominantly found in virulence factors of many pathogenic bacteria such as *L. monocytogenes*, *Yersinia* sp, *Shigella flexneri* and *Salmonella* sp. (Khodayari et al., 2010; Zaccari and Anderson, 2003). So, the lack of experimental NMR data motivated us to calculate NMR shielding tensors of nitrogen and oxygen atoms of aromatic β–sheet residues and compare the range of shielding shifts in a wide range of solvents encompassing a broad spectrum of polarity and hydrogen-bonding properties.

In the next step, because of broad host range of *L. monocytogenes* to infect over 40 species of wild and domesticated animals besides human and its survival in various environments, it was hypothesized that temperature is an important factor in InlB expression and invasion. So, thermochemical parameters of β-sheet of EGD strain–serovar 1/2A (PDB code = 1H6T) such as entropy, enthalpy and Gibbs free energy was calculated at different temperatures, that this bacterium may be encountered in the environment and in cold-blooded animals (25°C) or warm-blooded hosts (37 and 42°C) in three solvent media (McGann et al., 2007).

COMPUTATIONAL METHODS

These computer simulations provide a microscopic view of the important molecular events in atomic details and complement the macroscopic views of the experimental

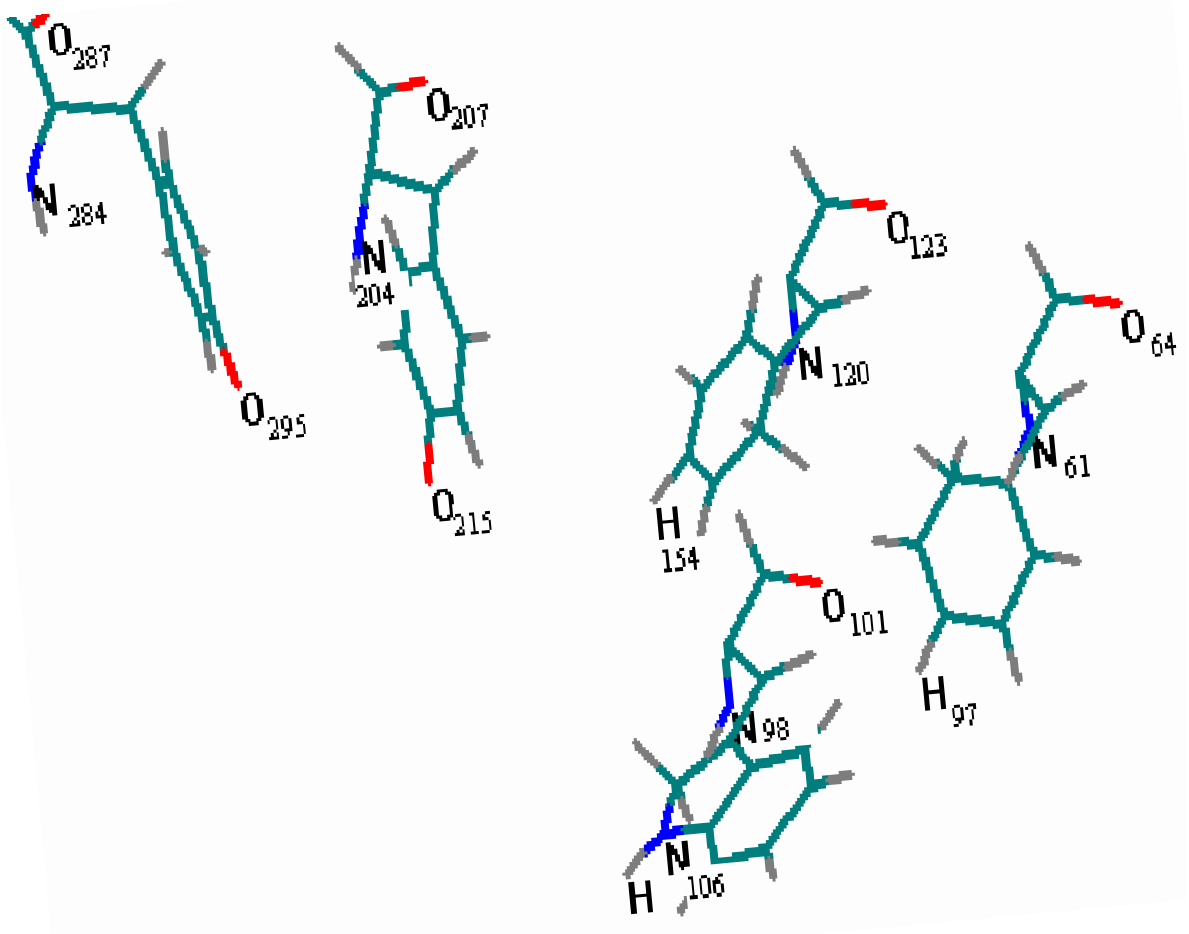

Figure 1. β-sheet molecular structure used for the analysis.

processes as well as open up practical strategies to discover novel therapeutics and protein-based drug design to combat this insidious bacterium.

The three-dimensional structure of InlB LRR, was taken from the X-ray coordinate file (Protein Data Bank (PDB) entry code: 1H6T). The coordinates of the amino acids distributed in seven tandem β-strands (residues 4 to 6 in each repeat), were selected and aligned respectively (Schubert et al., 2001). Hydrogen atoms which were not included in the PDB file were generated by the standard MM procedures. In order to conduct a thermodynamic investigation on modular structure of LRR domain, we constructed three fragments of β-sheets that is introduced by part A (2 first β-strands), part B (2 second β-strands) and part C (three third β-strands). Breaking bonds and gaps between strands were saturated by dummy atoms. In Figure 1, the concave face of β-sheet and linear arrangement of aromatic rings are shown and the atom numbering of five aromatic amino acids used throughout the text is included. After preparing appropriate models, all fragments were optimized with STO–3G, 3–21G and 6–31G(d,p) basis sets in the gas phase at the Hartree–Fock (HF) level of theory, to determine the molecular geometry with the GAUSSIAN 98 suite of programs adapted to a personal computer (Marino et al., 2000). Consequently, for estimating solvent effects on the conformational equilibrium and geometry, in comparison with gaseous phase as well as to appreciate the importance of solvent dielectric constant and polarity on solute-to-solvent interactions, the HF/SCRF calculations were performed. Six solvents with various dielectric constants: ε = 78.39, 46.8, 32.63, 24.55, 20.7, 7.58, corresponding to water, DMSO, methanol, ethanol, acetone and TetraHydroFuran (THF), respect-tively, were used. The simplest SCRF model is based on the Onsager's reaction field theory of electrostatic solvation. In this model, the solvent is considered as a uniform dielectric with a given dielectric constant (ε). The solute is assumed to occupy a spherical cavity of radius a_0 inside the solvent. The permanent dipole moment or higher electric multiple moments of the solute will induce a multiple in the surrounding medium, which will interact with the permanent molecular dipole, influencing the electronic structure of the solute. Firstly, the cavity radiuses for the SCRF calculations were determined from the estimated molecular volume of the three fragments.

Table 1. Calculated total energies E (in kcal/mol), dipole moments μ (in Debye) of β-sheet parts in different dielectric constants (ε) at the HF/6-31G(d,P) level of theory.

ε	E(kcal/mol) μ (Debye)					
	Vacuum **1**	**Water** **78.39**	**DMSO** **46.8**	**Ethanol** **24.55**	**Acetone** **20.7**	**THF** **7.58**
Part A	-1520373.916 8.672	-1520373.917 8.670	-1520373.921 8.676	-1520373.951 8.724	-1520373.973 8.759	-1520375.157 10.657
Part B	-1531379.36 4.3	-1531379.361 4.3045	-1531379.362 4.3049	-1531379.369 4.3364	-1531379.375 4.3591	-1531379.685 5.601
Part C	-2298427.436 8.659	-2298426.872 8.96	-2298426.876 8.97	-2298426.908 9.06	-2298426.933 9.13	-2298429.461 13.08

Then, the solvation calculations were performed at HF/6-31G (d,p) level using Onsager model (Huzinaga et al.,1984; Quinones et al., 2000).The numbers of atoms for the three fragments A, B and C were as 92, 97 and 126, respectively. So it took approximately 120 h to do the calculations. Frequency calculations, in order to appreciate thermo-chemical parameters such as Gibbs free energies, enthalpies and entropies of the molecule and a comparison of the obtained resultants with the aforementioned calculations were performed at four different temperatures: 298, 310, 315, 322k in aqueous phase and two other solvents (DMSO and THF). These may have significance for our understanding of β–sheet (un)folding and other biomolecular processes. To gain further insight into the solvent dielectric constant effects on important biomolecular mechanisms at the atomic level, NMR shielding tensors (ppm) of nitrogen and oxygen atoms of aromatic β–sheet residues have been computed with the continuous set of the gauge independent atomic orbital (GIAO) method with 6–31G(d,p) basis set (Monajjemi et al., 2005, 2006). NMR shielding tensors and magnetic susceptibilities using the Hartree–Fock theory computed with the GIAO method do not require large basis sets to achieve accurate results and systematically provide good results (Gao et al., 2007).

RESULTS AND DISCUSSION

With the various *ab initio* methods, one can obtain meaningful values for the contribution of one type of interaction or one chemical group to stability. As more detailed data became available, especially about the strength and specificity of non–covalent intra and inter molecules interactions at the atomic level, these events can be controlled more towards desirable directions. In addition, structure-based drug design begins with the deeper characteristic identification of ligand binding site on the target molecule.So we investigated the characteristic and (un) folding properties of InlB β–sheet and its aligned aromatic amino acids as a bacterial ligand, thermo chemically (Figure 1). Due to the prevalence of surface molecules in *L. monocytogenes* harboring the internalin domain, our results offers hope of developing methods leading to an increase in the resistance to *Listerial* infections.

β–Sheet conformation in vacuum and solvent

Initially, three fragments were optimized at the HF level with 6 to 31G basis set. The HF optimized parameters were used as initial input for subsequent HF/SCRF calculations. Predicted total energies and dipole moments of three parts are given in Table 1.

At the first glance, it is demonstrated that the total energy values of two β–stranded–parts A and B in water solvent are close to each other and as the number of strands increased in part C, the stability was done. The solvent effects on the energies of organic compounds are often well related to the dielectric constant (ε) of the solvent. The solute is treated as a low dielectric cavity in a high dielectric medium (Monajjemi et al., 2003). Solvent effects on the electronic structure of these fragments are manifested in the changes in atomic charges as well as in the increase in the dipole moment on going from the solvent of higher ε to lower ε. It means that the transfer of molecules from high-polar to low-polar solvents is culminated to instabilities. Normally, there is a charge distribution alongside the β–sheet, thus, increasing trend of dipole moment is indicative of focused electron clouds and somehow denaturation. In other words, the physical properties of three β-sheet parts in low–polar solvents on essentially similar scaffold are disrupted and these results indicate that there is direct correlation between dipole moment and the order of instability under SCRF conditions. As shown in Table 2, with decrease of

Table 2. Calculated relative thermochemical parameters: enthalpy ΔH, Gibbs free energy ΔG and entropy ΔS (in kcal/mol) of β-sheet parts in 4 temperatures (in Kelvin) and 3 solvents.

Temperature (K)	Part B (Trp124-Phe126) Part C (Tyr170-Tyr214)		
	ΔH	**ΔG**	**ΔS**
Water			
298	-678040.2565 -688498.4376	-678092.7599 -688548.3371	0.176114 0.167368
310	-678039.2584 -688497.4988	-678094.8664 -688549.3388	0.179393 0.170454
315	-678038.8289 -688497.0941	-678095.7669 -688550.1947	0.18077 0.171749
322	-678036.6124 -688495.193	-678098.9886 -688553.4033	0.183694 0.176555
DMSO			
298	-678040.255 -688498.4376	-678092.7561 -688548.3371	0.176093 0.167368
310	-678039.2579 -688497.4988	-678094.8626 -688550.3388	0.179472 0.170553
315	-678038.8274 -688496.9941	-678095.7625 -688551.1941	0.180775 0.172748
322	-678035.5 143 -688495.1193	-678098.7261 -688554.4027	0.184112 0.177213
THF			
298	-678040.2374 -688498.4244	-678092.7141 -688548.2976	0.176129 0.167478
310	-678039.2409 -688497.4856	-678094.8193 -688550.298	0.179563 0.170564
315	-678038.8105 -688496.7754	678095.7192 -688551.1533	0.180990 0.172859
322	-678035.198 -688495.0061	-678098.9905 -688554.8027	0.184812 0.177761

dielectric constant, the values of Gibbs free energies became more positive, too. This reinforces the opinion that the molecules in polar solvents is more stable than in low–polar solvents, which is in agreement with the aforementioned conclusions. According to Table 1, the molecule has the most stability in water and the shifts

obtained in dipole moment for polar solvents are relatively closed to each other and gradually towards the low-polar solvents, the deviations will be more pronounced in the THF, where there is least stabilities. The solvation energy calculated by the SCRF method corresponds to the electrostatic contribution of the free energy of salvation. This method, evaluates only the electrostatic component of solvation (Monajjemi et al., 2003). Most of the β–sheets fold with an identifiable core of hydrophobic residues which in the case of InlB β–sheet, is more significant (Monajjemi et al., 2011; Main et al., 2005). Lazaridis and Karplus (2003) reported that the electrostatic solvation energies in unfolded state are more negative primarily because back–bone hydrophobic hydrogen bonding groups buried in the native state become more exposed to the solvent. Thus, these buried hydrophobic groups have become accessible in low–polar solvents, culminating to protein unfolding and the negative trend which is seen in total energies from water to THF is a representative of the unfolding of the molecule, too. Thus, there are the least stabilities in THF. As it appeared, all the conclusions are in a good agreement with each other.

Temperature and solvent effects on the β–sheet (un)folding and thermo chemical functions

Non–covalent interactions play a key role in protein folding and specificity of ligand–receptor bonding (Main et al., 2005). As discussed earlier, the interfaces between β–strands are saturated by hydrogen bonds in whole β–sheet, which can affect the thermo-chemical behavior of the molecule. The string of aromatic amino acids, located at the concave surface of the LRR domain was considered as a hot-spot for InlB–Met binding and thermo-chemical parameters of Trp124–Phe126 in part B and Tyr170–Tyr214 in part C were assayed in four temperatures and solvents such as water, DMSO as well as THF and reported, in Table 2.

Comparison of Gibbs free energies in different solvents at four temperatures demonstrates that the molecule has the most negative values of ΔGs in water than DMSO and THF, respectively indicative of (1): dominant role of water in biomolecular systems in which stability of the molecule in water is at most and (2): decrease of dielectric constant value leading to more destructive effect on molecule. So, THF, which has the least polar solvent causes higher structural changes and protein unfolding at the earlier mentioned temperatures.

Unlike intramolecular enthalpies, solvation enthalpies are highly temperature- dependant and the enthalpy of unfolding becomes progressively more endothermic with increasing temperature (Lazaridis and Karplus, 2003). In lower temperatures, H-bonds between strands, within the structure, can be relatively preserved or likely replaced by H-bonds to water molecules. So, little deviation is observed in thermo-chemical parameters particularly in terms of free energy (ΔG). It can be concluded that these repetitive secondary structures, which stacked on each other with internal hydrogen bonded network, regardless of increasing temperature up to 42°C can remain relatively intact, especially in the hot–spot region. However, at 49°C the values of enthalpy become more positive and endothermic and ΔG and entropy values show tangible deviations, too. These are indicative of protein unfolding. Some researchers used differential scanning microcalorimetry (DSC) for investigating stability of InlB248 and InlB321, and reported that endothermic denaturation transitions are around 42 and 49°C ,respectively (Courtemanche and Barrick, 2008). Our finding, in hot spot region in water is identical with our studies of thermal effect on InlB321. We hypothesized that the role of polar solvents, particularly water in the overall thermodynamics of such a system which is a non–covalent–weaked interactions like hydrogen bonds have crucial role in controlling folding, is so dominant and temperature dependent, and because of the unusual properties of water molecules with large heat capacity, it can inhibit quick thermal denaturation of this system (Lazaridis and Karplus, 2003).

In a previous study, Courtemanche and Barrick (2008) found that the LRR domain of InlB has two–state equilibrium folding and unfolding pathways. With rise in temperature up to 49°C, following more buried hydrophobic group exposure and increased freedom degrees of molecule, H-bonds in the protein-water system is going to break and the disordered liquid state reinforces thermal disruption of intermolecular H-bonds which could be held in place by the cooperatively hydrogen bonded network. Consequently, β–sheet unfolds all at once. The comparison of two studied parts reveals that both of them follow the same thermo-chemical patterns in explained temperatures and solvents. These are consistent with the earlier–mentioned notion about the equilibrium two-state (un)folding pathways, reported by Courtemanche and Barrick (2008). So, it seems that there is a cooperation among the β–strands thermodynamically in which taken together the whole β–sheet thermodynamics character is determined.

NMR structural studies in different media

Although, the structure of InlB has already been determined by X–ray crystallography, NMR assignments, based on the quantum mechanical property of nuclei are valuable, because it can be used to probe InlB–Met (ligand–protein) binding via clarifying of chemical shift mapping and dynamics. On the other side, it is often desirable to compare chemical shifts variations, obtained under some conditions such as different solvents, and changes in solvent polarity may influence intermolecular shielding of InlB β–sheet.

Typically, three principal Eigen values (σ_{11}, σ_{22}, σ_{33}) and the isotropic value (σ_{iso}) as well as the anisotropy of the tensor (σ_{aniso}) can be predicted by suitable quantum mechanical computations (Harris et al., 2008) in order of increasing shielding as:

$$\sigma_{11} \leq \sigma_{22} \leq \sigma_{33} \quad (1)$$

the definition of isotropic shielding, σ_{iso}, is clearly:

$$\sigma_{iso} = \frac{1}{3}(\sigma_{11} + \sigma_{22} + \sigma_{33}) \quad (2)$$

It is useful to express shielding tensor data using three other parameters as well as the principal components. One of these is shielding anisotropy tensor ($\Delta\sigma$):

$$\Delta\sigma = \sigma_{33} - \frac{1}{2}(\sigma_{11} + \sigma_{22}) \quad (3)$$

The second parameter is referred to as chemical shift (δ):

$$\delta = \sigma_{33} - \sigma_{iso} \quad (4)$$

The third component is shielding asymmetry (η), is defined as (Harris et al., 2008):

$$\eta = \frac{|\sigma_{22} - \sigma_{11}|}{|\sigma_{33} - \sigma_{iso}|} \quad (5)$$

Table 3 provides results for NMR shielding tensors (ppm) of aromatic amino acids ^{15}N and ^{17}O in vacuum, water, DMSO, ethanol and THF. Based on calculations with Equations (1) to (5), It is worth noting that there is only a small dependence of the nuclear shielding on the various environments and the solvents employed is likely to enter into rather weak molecular interactions with the solutes in which a small change in chemical shift values is seen while going from gaseous to liquid phase environment.

These results can be indicative of (1): rigidity of this unit, packing more closely which is clearly an advantage for a molecule exposed to the hostile proteolytic host environment. As a result, it can easily accommodate a large range of repeats, between six LRRs in InlC to 15 LRRs in InlA (Tsai et al., 2006) and (2): the experimental data are suitable for comparing with theoretical values of the nuclear shielding calculated for this isolated molecule. Nevertheless, gas to solution shifts of the N120 in Phe126 amino group and O101 in Trp124 carboxyl group shielding are relatively more pronounced. In addition, the shielding variations of the ^{15}N and ^{17}O atoms involved in aromatic rings are relatively larger.

This can be due to, (1); most exposure of them in solvent media and, (2); well-known ring current effects. So, their chemical shifts are much more sensitive to the local environment than that of oxygen and nitrogen atoms, engaged in the backbone carboxyl and amino groups. It was shown that the hydrogen bonding of THF with NH of the Trp indole ring has more effect on the nitrogen chemical shift, consequently significant effect on the electronic configuration of indole and then amino acid. On the other hand, the downfield movement in chemical shift seems to arise from increasing delocalization of the nitrogen electron lone pairs by the π–electron system which results in increased anisotropic deshielding with the decreasing polarity of the medium and the most density changes, is resulted from the interaction with THF. The extension of π resonance system in indole ring can play a considerable role in this behaviour, too. The only exception is that DMSO induces the least chemical shift in Trp–indole–N atom. The trends in Tyr–phenol–O atoms are inversed (Figure 2a) and are related to hydrogen bond donor strength of solvent, in which the most anisotropic deshielding values are observed in water. In addition, it seems that the delocalization of electron lone pairs is augmented by solvent polarity. These characters are likely more stressed by forming partial double bond of the C–O bond on aromatic ring induced by π–resonance system. It is to be noted that Tyr214–O ring has the maximum chemical shift values, in all the environments regarding to the Tyr170–O ring.

The insignificant chemical shifts of nitrogen and oxygen atoms engaged in the backbone of carboxyl and amino groups can be due to 1: strong intramolecular H–bonds that impede the formation of intermolecular H–bonds and 2: regarding to the aromatic rings atoms, they are positioned at the internal surface of the amino acids, that is thereby affected by solvents weakly. In other words, ^{15}N and ^{17}O atoms shielding of aromatic rings, are more likely to be solvent dependent but the possibility of solute-to-solvent hydrogen bond effects on the other nitrogen and oxygen atoms are weaker. The N-amino groups and O–carboxyl groups shielding of both Tyr–170 and Tyr–214 show similar changes in the aforementioned environments.

However, the shielding variation of ^{15}N atoms seems to follow the polarity of solvent in the sense of enhanced deshielding, with the increasing polarity. Although, the increasing hydrogen bond donor strength of solvent, produces a low deshielding effects on them. These trends for ^{17}O atoms are inversed and they are more shielded in polar solvents (Figure 2b and c).As shown in Figure 2b and c, the hydrogen bond donor strength of solvent has quite insignificant effect on N120, O101 and O123, and aprotic solvents like DMSO and THF produced more deshielding effects on them.

Conclusion

At first glance, *ab initio* HF calculations, obtained a good

Table 3. NMR shielding values of ^{15}N and ^{17}O (in ppm) calculated for aromatic amino acids at HF/6-31G level of theory in vacuum and solvent media.

Atom	Gas phase										
	Phe126		Trp124				Tyr170			Tyr214	
	N120	O123	N106	O101	N98	O215	N204	O207	O295	N284	O287
σiso	-119.104	-408.0687	222.1179	-380.4835	-115.848	-284.509	-146.3503	-425.3974	-339.5922	-144.6704	-391.828
σaniso	568.9443	1222.095	98.9124	1179.4304	565.6336	1001.5224	600.4745	1255.7634	1099.4062	593.8487	1200.189
Δσ	-606.592	1222.095	98.91235	1179.4304	-602.138	1001.52235	-680.7795	1255.7634	1099.4062	-670.8102	1200.189
η	0.87587	0.63376	0.123076	0.617318	0.87875	0.674712	0.764079	0.63176	0.722086	0.77054	0.621115
δ	-404.3945	814.73	65.9416	786.287	-401.426	667.6816	-453.853	837.1756	732.9375	-447.2068	800.126
ε	**Water**										
σiso	-118.097	-407.6058	222.1715	-379.9448	-115.900	-284.5595	-146.3498	-425.4185	-339.5758	-144.6139	-391.8638
σaniso	567.802	1221.1996	98.9749	1178.7672	565.8846	1001.6416	600.4589	1255.7949	1099.3839	593.8107	1200.2698
Δσ	-604.545	1221.1995	98.97945	1178.76715	-602.091	1001.6416	-680.785	1255.7949	1099.3839	-670.7473	1200.2698
η	0.87844	0.63333	0.121318	0.617522	0.87973	0.674746	0.764019	0.631787	0.722077	0.770594	0.621103
δ	-403.030	814.133	65.9863	785.8448	-401.393	667.761	-453.857	837.1966	732.9226	-447.1649	800.1799
ε	**DMSO**										
σiso	-118.3877	-407.778	222.1349	-380.1288	-115.960	-284.5577	-146.3513	-425.4298	-339.5759	-144.6134	-391.8696
σaniso	568.2067	1221.49	98.9084	1179.0165	565.8718	1001.636	600.4589	1255.8092	1099.3823	593.8089	1200.2815
Δσ	-605.188	1221.490	98.9084	1179.0165	-602.257	1001.6361	-680.7954	1255.8093	1099.3823	-670.752	1200.2816
η	0.87778	0.63354	0.122316	0.61744	0.87917	0.6747353	0.76399	0.6317936	0.722069	0.770577	0.621117
δ	-403.459	814.3266	65.939	786.011	-401.505	667.7574	-453.8636	837.2062	732.9215	-447.168	800.1877
ε	**Ethanol**										
σiso	-118.156	-407.6187	222.2632	-379.9643	-115.934	-283.4939	-146.3548	-425.5142	-339.3805	-144.6059	-391.9049
σaniso	567.8874	1221.236	99.1346	1178.7883	565.9116	999.0226	600.4286	1255.9279	1098.621	593.7865	1200.3334
Δσ	-604.670	1221.236	99.1341	1178.7883	-602.158	999.0226	-680.8252	1255.9279	1098.62105	-670.7384	1200.3334
η	0.878338	0.633337	0.120425	0.6175	0.879612	0.671773	0.763826	0.631872	0.719928	0.770546	0.621156
δ	-403.114	814.1574	66.2452	785.8589	-401.439	666.0151	-453.8834	837.2853	732.4141	-447.1589	800.2223
ε	**THF**										
σiso	-119.8449	-407.5723	222.6821	-380.2773	-116.586	-282.1324	--146.3702	-427.9761	-339.1012	-144.4749	-393.3879
σaniso	570.7951	1221.7141	99.8112	1179.0267	566.7048	997.5631	599.6511	1259.1867	1097.732	593.0569	1203.0302
Δσ	-608.024	1221.71415	99.8112	1179.0267	-603.418	997.563	-681.990	1259.1867	1097.7321	-671.297	1203.0302
η	0.87754	0.632606	0.11957	0.61661	0.878316	0.669681	0.758535	0.6337908	0.70222	0.766897	0.622412
δ	-405.35	814.4862	66.7661	786.0178	-402.279	665.234	-454.660	839.4578	731.5431	-447.5317	802.0201

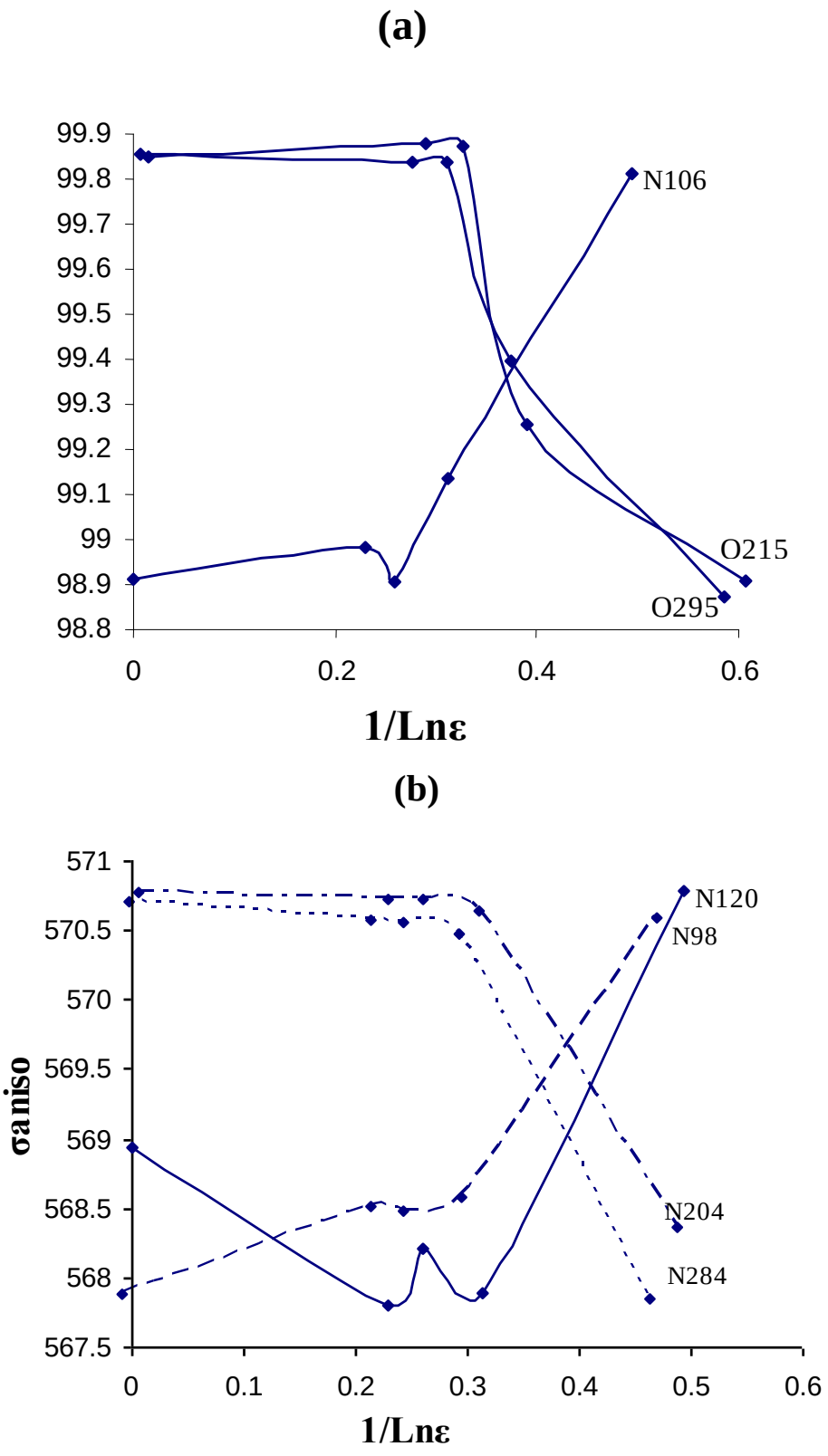

Figure 2. The graphs of (a) shielding anisotropy tensors of Trp-indole-^{15}N and Tyr-phenol-^{17}O atoms, (b) anisotropy shieldings of amino groups- ^{15}N and (c) shielding anisotropy tensors of carboxyl groups- ^{17}O in mentioned aromatic amino acids (in ppm) for different values of the dielectric constant [1/Lnε] at the 6-31G level of theory in the basis of GIAO method.

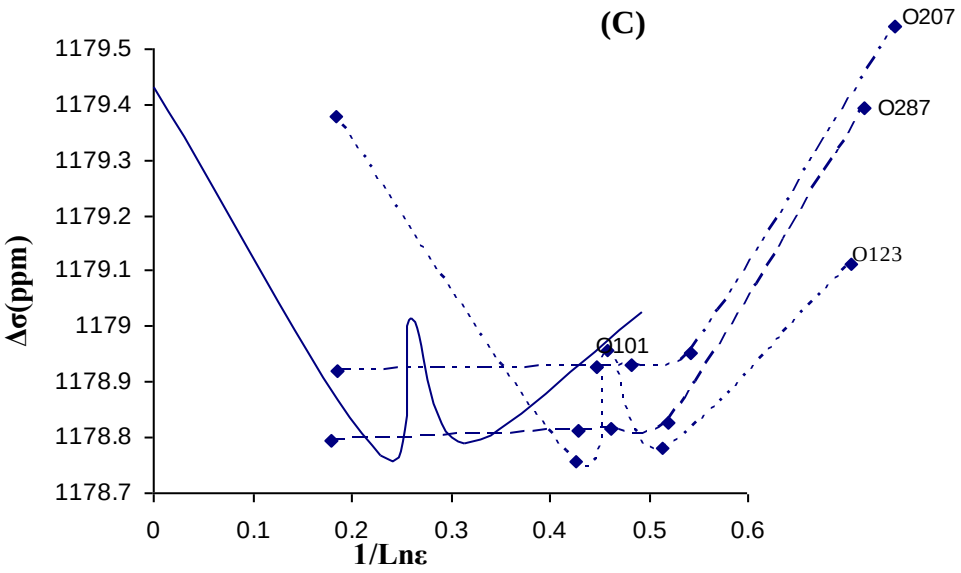

Figure 2. Contd.

agreement by the presented experimental data. Also, these calculations predict a relatively significant independence of the isolated InlB β–sheet geometry on the environmental effects especially in polar solvents. These are in accord with the notion that InlB exists in two forms, non–covalently associated with the bacterial surface and free in solution, and also high-affinity binding event between concave face of the molecule and Met is necessary for internalization of bacteria. However, this molecule varies mostly in the solvents by low dielectric constants like THF at 49°C and there is cooperation among β–strands, thermodynamically. On the other hand, the aromatic rings atoms especially Trp–indole–N and Tyrs–phenol–O atoms are more affected by local environment like varieties in dielectric constant and solvent polarity.

On the other side, InlB β–sheet was viewed as islalnds of cooperatively-ordered hydrogen-bonded structure, and the role of water molecules in the overall thermodynamics is significant and highly temperature dependent. It seems that in unfolding and even in its ligand–dissociation processes (with the notion that hydrogen bonds have the essential role in Met–residues binding) (Niemann et al., 2007), H–bonds between protein groups would be replaced by H–bonds to water and the role of water molecules in controlling properties of this rigid unite is of great importance. Thereby, the unique, packed and exposed linearly arrangement of aromatic rings with a variety of potential hydrogen bond donors and acceptors, with a small size can be an ideal part for drug design.

REFERENCES

Cabanes D, Dehoux P, Dussurget O, Frangeul L, Cossart P (2002). Surface proteins and the pathogenic potential of *Listeria monocytogenes*. Trends Microbiol. 10: 238-245.

Chatterjee S, Otten S, Hain T, Lingnau A, Wehland J, Domann E, Charkraborty T (2006). Invasiveness is a variable and heterogeneous phenotype in *Listeria monocytogenes* serotype strains. Internat. J. Med. Microbiol. 296: 277-286.

Cossart P (2002). Molecular and cellular basis of the infection by *Listeria monocytogenes*: an overview. Int. J. Med. Microbial. 291: 401-409.

Cossart P, Pizarro-Cerda J, Marc, Lecuit M (2003). Invasion of mammalian cells by *Listeria monocytogenes*: functional mimicry to subvert cellular functions. Trends Cell Biol.13: 23-31.

Courtemanche N, Barrick D (2008). Folding thermodynamics and kinetics of the leucine-rich repeat domain of the virulence factor Internalin B. Protein Sci. 17: 43-53.

Donald BR, Martin J (2009). Automated NMR assignment and protein structure determination using sparse dipolar coupling constraints. Progress Nuclear Magnetic Resonance Spectroscopy, 55: 101-127.

Freiberg A, Machner PM, Pfeil W, Schubert WW, Heinz D, Seckler R (2004). Folding and stability of the leucine-rich repeat domain of internalin B from *Listeria monocytogenes*. J. Mol. Biol. 337: 453-461.

Gao Qi, Yokojima S, Kohno T, Ishida T, Fedorov DG, Kitaura K, Fujihira M, Nakamura SH (2007). Ab initio NMR chemical shift calculations on proteins using fragment molecular orbitals with electrostatic environment. Chem. Phys. Lett. 445: 331-339.

Harris R, Becker E, Menezes S, Granger P, Hoffman R, Zilm K(2008). Further conventions for NMR shielding and chemical shifts. Solid State Nuclear Magnetic Resonance. 33:41-56.

Huzinaga S, Andzelm M, Klobukowski M, Radzio-andzelm E, Sakai Y, Tatewaki H (1984). Gussian basis set for molecular calculations. Elsevier, Amesterdam.

Khodayari F, .Mollaamin M, Monajjemi (2010). Structural changes of DHA-containing phospholipids by K+ and Na+ cations in nerve cell membranes . Afr. J. Microbiol. Res. 4: 1282-1290.

Lazaridis TH, Karplus M (2003). Thermodynamics of protein folding: a microscopic view. Biophys. Chem. 100: 367-395.

Machner MP, Frese S, Schubert WD, OrianRousseau V, Gheradi E, Wehland J, Niemann HH, Heinz DW (2003). Aromatic amino acids at the surface of InlB are essential for host cell invasion by *Listeria monocytogenes*. Mol. Microbiol. 48(6): 1525-1536.

MainRGE, Lowe A, Mochrie S, Jackson S, Regan L (2005). A recurring theme in protein engineering: the design, stability and folding of repeat proteins. Curr. Opin. Structural Biol. 15: 464-471.

Marino M, Banerjee M, Jonquieres R, Cossart P, Ghosh,P (2002). GW domains of the *listeria monocytogenes* invasion protein InlB are SH3-

like and mediate binding to host ligands. EMBO J. 21: 5623-5634.
Marino M, Braun L, Cossart P, and Ghosh P (2000). Framework for interpreting the leucine-rich repeats of the Listeria internalins. Proc. Natl. Acad. Sci. USA. 97: 8784-8788.
Marino M, Braun L, Cossart P, Ghosh P (2000). A framework for interpreting the leucine-rich repeats of the Listeria internalins. Proc Natl Acad Sci U S A. 97(16):8784-8
McGann P, Ivanek R, Wiedmann M, Boor KJ (2007). Temperature-dependent expression of *Listeria monocytogenes* internalin and internalin-like genes suggests functional diversity for these proteins among the listeria. Appl. Environ. Microbiol. 73: 2806-2814.
Mollaamin F, Layali I, Ilkhani AR, and Monajjemi M (2010). Nanomolecular simulation of the voltage–gated potassium channel protein by gyration radius study. Afr. J. Microbiol. Res. 4: 2795-2803.
Mollaamin F, Shahani Poor K, Nejadsattari T, and Monajjemi M (2010). Bio-nanomodeling of active site in oxidized azurin using by computational methods. Afr. J. Microbiol. Res. 4: 2098-2108.
Monajjem M, Ketabi S, Amiri A(2006). Monte Carlo Simulation Study of Melittin: Protein Folding and Temperature Dependence. Russian J. Phys. Chem. 1: 55-62.
Monajjemi M, Chahkandi B (2005). Theoretical investigation of hydrogen bonding in Watson-Crick, Hoogestein and their reversed and other models: comparison and analysis for configurations of adenine-thymine base pairs in 9 models, J. Mol. Structure Theochem. 714: 43-60.
Monajjemi M, Ghiasi R, Abedi A (2005). Theoretical investigation of the interaction of cytosine and its tautomers with alkali Metals. Russian J. Inorganic Chem. 50: 382-388.
Monajjemi M, Honarparvar B, Haeri H, and Heshmat M (2006). An ab-initio quantum chemical investigation of solvent induced effect on N-NQR parameters of Alanine,Glycine,Valine and Serine using Polarizable Continuum Model. Russ. J. Phys. 80: 40-44.
Monajjemi M, Mollaamin F, Gholami MR, Yoosbashizadeh H, Sadrnezhad SK, Passdar H (2003). Quantum chemical parameters of some organic corrosion inhibitors, pyridine, 2-picoline 4-picoline and 2,4-lutidine, adsorption at aluminum surface in hydrocholoric and nitric acids and comparison between two acidic media. Main Group Metal Chem. 26: 349-361
Monajjemi M, Movahedi M, Mollaamin F (2011). Quantum mechanic studies on dipalmitoylphosphatidylcholine and dimyristoylphosphatidylcoline as nanoscales of membrane. Afr. J. Microbiol. Res. 5: 250-259.
Niemann HH, Jager V, Butler JG, Heuvel J, Schemidt S, Ferraris D, Gherardi EW, Heinz DW (2007). Stucture of the human receptor tyrosine kinase Met in complex with the Listeriainvasion protein InlB. Cell. 130: 235-264.
Patel MA, Deretey E, Csizmadia IG (1999). Will ab initio and DFT drug design be practical in the 21st century? A case study involving a structural analysis of the β_{2-} adrenergic G-protein coupled receptor. J. Mol. Structure Theochem. 492: 1-18.
Pishkar L, Monajjemi M, Ilkhani AR, Mollaamin F (2010). Theoretical investigation of dielectric effects on Nanostructure of - amyloid peptide. Int. J. Phys. Sci. 5: 1450-1464.
Quinones E, Ishikawa Y, Leszczynski J (2000). Conformational properties of dimethylaminobenzonitrile in gas phase and polar solvents: ab initio HF/6-31G (d,p) and MP2/6-31G(d,p) investigations. J. Mol. Structure Theochem. 529: 127-134.
Schubert W,Gobe G, Diepholz M (2001). Inls from the human pathogen *listeria monocytogenes* combine three distinct folds into a contiguous internalin domain. J. Mol. Biol. 312: 783-794.
Shen Y, Naujokas M, Park M, Ireton K (2000). InlB-dependent internalization of Listeria is mediated by the Met receptor tyrosine kinase. Cell. 103: 501-510.
Tsai Y, Orsi R, Nightingale K, Wiedmann M (2006). *Listeria monocytogenes* internalins are highly diverse and evolved by recombination and positive selection. Infect. Genet. Evol. 6: 378-389.
Zaccari C, Anderson A (2003). The process of structure-based drug design. Chem. Biol. 10: 787-797.